

# SIMULATION OF THE APS-U ORBIT MOTION DUE TO RF NOISE\*

V. Sajaev, ANL, Argonne, IL, USA

## Abstract

The APS Upgrade storage ring will keep the same rf system that is presently used at APS. This rf system has amplitude and phase noise dominated by the lines at 60, 180, and 360 Hz. APS presently operates with a synchrotron frequency close to 2 kHz, which is far away from the rf noise frequencies, yet still the rf system noise contributes over 2  $\mu\text{m}$  rms to the horizontal orbit noise due to beam energy variation. APS-U will operate with a bunch-lengthening cavity, which will lower the synchrotron frequency to about 200 Hz. This could potentially lead to large orbit noise and other negative consequences due to energy variation caused by the rf system noise. In this paper we will present simulations of the rf noise-induced orbit motion at APS and APS-U, then define the rf amplitude and phase noise requirements that need to be achieved for APS-U operation.

## INTRODUCTION

APS-U [1] will have the same RF system [2] that is now used at APS. Figure 1 shows the measured rms phase and amplitude noise of the APS rf system obtained by integrating the Power Spectral Density (PSD). This measurement was performed a few years ago by T. Berenc [3]. Two rf systems are shown; the noise characteristics for them are similar. One can see that the dominating contributor in the phase noise is 360 Hz line. For amplitude, several lines contribute, mainly 60, 180 and 360 Hz.

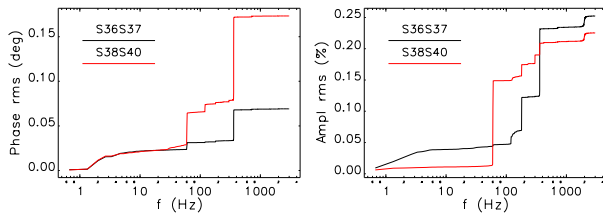


Figure 1: Measured phase (left) and amplitude (right) rms noise for APS rf systems (2017 measurement).

To determine how much of the orbit motion at 360 Hz is contributed by rf-induced energy variation, one can extract the beam energy variation from the orbit motion as follows:

$$\frac{\delta E}{E}(t) = \frac{\mathbf{x}(t) \cdot \boldsymbol{\eta}}{\boldsymbol{\eta} \cdot \boldsymbol{\eta}}, \quad (1)$$

where  $\mathbf{x}$  is the vector of orbit and  $\boldsymbol{\eta}$  is the vector of dispersion. This expression is obtained from  $\mathbf{x} = \mathbf{x}_\beta + \boldsymbol{\eta} \delta E/E$  after scalar multiplying both sides by  $\boldsymbol{\eta}$  and assuming that the scalar product  $\mathbf{x}_\beta \cdot \boldsymbol{\eta}$  is zero. The rms beam energy error

\* Work supported by the U.S. Department of Energy, Office of Science, Office of Basic Energy Sciences, under Contract No. DE-AC02-06CH11357.

extracted this way is shown on Fig. 2 (left). The relative beam energy variation is dominated by 360 Hz line and totals  $\sim 1.2 \cdot 10^{-5}$ . Figure 2 (right) shows the total rms orbit motion, the energy-variation-induced rms orbit motion, and the remaining part of the orbit motion that was obtained by subtracting the energy-induced motion PSD from the total PSD. One can see that the entire orbit motion at 360 Hz is defined by the rf noise, and the total rms orbit motion rms near that frequency is 2.0  $\mu\text{m}$ .

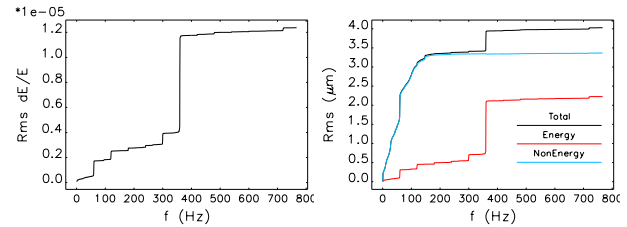


Figure 2: Left: Rms noise of the relative beam energy obtained using Eq. (1). Right: Orbit motion rms: total motion (black), energy variation induced motion (red), and the remaining motion (blue).

## CALCULATIONS FOR APS

Single particle tracking with elegant [4] was used to simulate the orbit motion due to rf noise. The tracking was performed for 20,000 turns to cover several synchrotron oscillations, and the `&modulate_elements` command was used to vary rf cavity phase during tracking. To calculate the rms noise of the closed orbit, the PSD of the particle coordinates was calculated and then integrated around the phase modulation frequency  $f_{\text{mod}}$ .

Synchrotron motion is a damped harmonic oscillator with resonant frequency equal to the synchrotron frequency  $\omega_s$  and quality factor  $Q$  equal to  $\tau_z \omega_s / 2$ , where  $\tau_z$  is the longitudinal damping time. The response of the oscillator to the excitation can be described by the following expression, which gives the ratio of the oscillation amplitude  $u$  to the amplitude of the excitation  $u_0$  as a function of the modulating frequency  $\omega_{\text{mod}}$  [5]:

$$\frac{u(\omega_{\text{mod}})}{u_0} = \frac{\omega_{\text{res}}^2}{\sqrt{(\omega_{\text{res}}^2 - \omega_{\text{mod}}^2)^2 + \left(\frac{\omega_{\text{res}} \omega_{\text{mod}}}{Q}\right)^2}}. \quad (2)$$

The beam time of arrival and energy variation can expressed using rf phase  $\varphi$  as follows [6]:

$$\delta t = \frac{\Delta \varphi}{\omega_{\text{rf}}}, \quad \frac{\delta E}{E} = -\frac{\dot{\varphi}}{\omega_{\text{rf}} \alpha_c}, \quad (3)$$

where  $\alpha_c$  is a momentum compaction factor. Using Eqs. (2) and (3), one can write the amplitude of the beam

arrival time oscillation as a function of the phase modulation amplitude  $\Delta\varphi$ :

$$\widehat{\delta t}(\omega_{\text{mod}}) = \frac{\omega_s^2}{\sqrt{(\omega_s^2 - \omega_{\text{mod}}^2)^2 + \left(\frac{2\omega_{\text{mod}}}{\tau_z}\right)^2}} \frac{\widehat{\Delta\varphi}}{\omega_{\text{rf}}} \quad (4)$$

and the amplitude of the beam energy variation as

$$\frac{\widehat{\Delta E}}{E}(\omega_{\text{mod}}) = \frac{\omega_s^2}{\sqrt{(\omega_s^2 - \omega_{\text{mod}}^2)^2 + \left(\frac{2\omega_{\text{mod}}}{\tau_z}\right)^2}} \frac{\omega_{\text{mod}}}{\alpha_c \omega_{\text{rf}}} \widehat{\Delta\varphi}. \quad (5)$$

These expressions can now be compared with the simulation results. Figure 3 (left) shows the comparison of the Eq. (4) and simulation results for  $\delta t$ , while the plot on the right shows the comparison of the Eq. (5) with the simulation for  $\Delta E/E$ . Agreement for both quantities is very good, as tracking results are indistinguishable from the analytic expression. To test the model further, the rf voltage was scanned from 6.0 to 9.0 MeV, which would change the synchrotron frequency and the Q factor. In all cases, the agreement was as good as in Fig. 3.

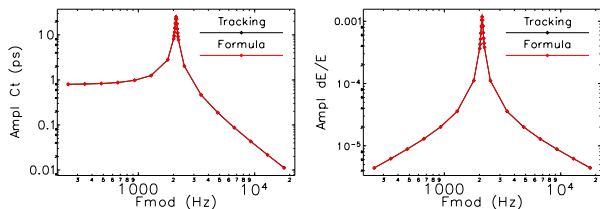


Figure 3: Left: comparison of tracking simulation and results predicted by Eq. (4) for  $\delta t$ . Right: comparison of tracking simulation and results predicted by Eq. (5) for  $\Delta E/E$ . The agreement in both cases is very good.

Now one can calculate the expected orbit motion rms due to slow rf phase modulation far from resonance. The Eq. (5) simplifies to

$$\frac{\widehat{\Delta E}}{E} = \frac{\omega_{\text{mod}}}{\alpha_c \omega_{\text{rf}}} \widehat{\Delta\varphi}. \quad (6)$$

Using phase noise at 360 Hz shown in Fig. 1 for S38S40 system ( $\Delta\varphi_{\text{rms}} = 0.15^\circ$ ), the expected rms orbit noise is  $1.7 \mu\text{m}$  at P2 BPMs ( $\eta_x = 0.18 \text{ m}$ ), which is close to the measured value of  $2.0 \mu\text{m}$  rms at 360 Hz shown in Fig. 2 (right).

## SIMULATIONS FOR APS-U

The main difference for APS-U will be the presence of the Higher-Harmonic Cavity (HHC) [7, 8] which is used to lengthen the bunch. The HHC lowers the synchrotron frequency and introduces the frequency dependence on the amplitude of the longitudinal oscillation [9]. The simple harmonic oscillator description would not work any more, so tracking simulations have to be used.

HHC tuning can be optimized for different purposes. For the simulations presented here, a “flat potential” condition will be used, because it can be clearly defined, and because this condition should not differ much from the maximum lifetime condition [10], in which APS-U HHC will operate. Due to the lower synchrotron frequency, more turns are needed for tracking compared to APS. In addition, a bunch of particles was tracked instead of a single particle to take possible decoherence effects into account. Specifically, 100k turns and 5k particles was used, and the one-turn lattice was represented by a single ILMATRIX element of elegant. Figure 4 shows the comparison of the average beam energy oscillation for a single particle and for a bunch of particles when rf phase is varied. It shows that decoherence does lead to about a factor of two reduction in the oscillation amplitude.

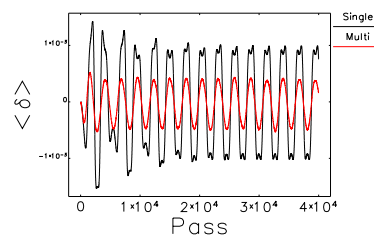


Figure 4: Comparison of single-particle and multi-particle tracking; decoherence in multi-particle tracking reduces the average energy oscillation amplitude by about a factor of two for the simulated  $0.2^\circ$ , 100-Hz phase oscillation.

A scan of modulating frequency  $f_{\text{mod}}$  for APS-U was performed using multi-particle tracking. Figure 5 shows the results for beam energy oscillation due to  $0.1^\circ$  rf phase oscillation or 0.2% rf voltage oscillation. One can see a broad resonance around 170 Hz. This resonance curve and noise shown in Fig. 1 were then used to calculate the expected relative beam energy noise using the S36S37 noise spectrum for amplitude and the S38S40 noise for phase (worst performers out of two systems were chosen to be conservative). Figure 6 (left) shows the expected rms beam energy noise. The total relative beam energy noise reaches  $4.7 \cdot 10^{-4}$ , while the beam energy spread is  $1.3 \cdot 10^{-3}$ . If one follows the same stability requirement as in transverse planes – 10% of the beam size – then the stability requirement for beam energy would be  $1.3 \cdot 10^{-4}$ . In this case, the noise shown in Fig. 1 exceeds the requirements by a factor of three.

Energy variation will result in orbit motion in locations with non-zero dispersion. Dispersion in APS-U ID straight sections is small but not zero. The expected dispersion can be found using commissioning simulations, which give the expected distribution of lattice functions after lattice correction with realistic errors [11]. The 95<sup>th</sup>-percentile value of dispersion was used for orbit motion calculations, which corresponded to  $1.5 \text{ mm}$  and  $6 \cdot 10^{-4}$  for dispersion and its slope in horizontal plane and  $1.0 \text{ mm}$  and  $4 \cdot 10^{-4}$  in vertical plane. Using these dispersion values and the total energy noise from Fig. 6 (left), one can calculate the

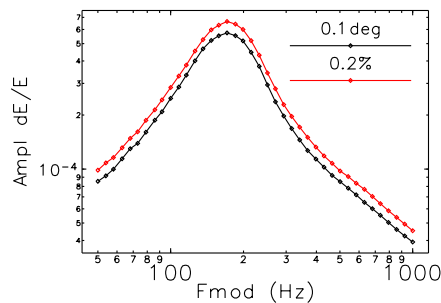


Figure 5: Simulated APS-U relative energy oscillation amplitude as a function of rf phase (black) and voltage (red) modulation frequency.

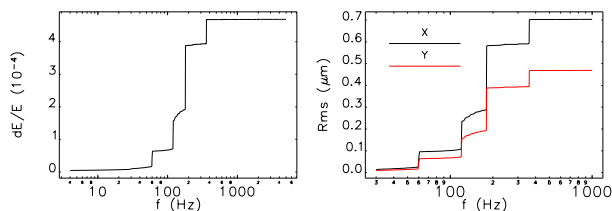


Figure 6: Left: Expected rms relative beam energy noise in units of  $10^{-4}$ . Right: Orbit rms noise resulting from the beam energy noise shown in the left plot.

expected orbit motion noise of  $0.7 \mu\text{m}$  and  $0.30 \mu\text{rad}$  in horizontal plane and  $0.5 \mu\text{m}$  and  $0.19 \mu\text{rad}$  in vertical plane. Vertical position and angle noise in both planes exceed the orbit stability requirements shown in Table 1. Spectra of the expected rms orbit motion are shown in Fig. 6 (right). These results do not take orbit correction into account because traditional orbit correction is not able to correct for the effect of beam energy noise. Special orbit correction that uses rf phase as one of its actuators could reduce this orbit effect and is under study for APS-U [12], but it was not considered here. In the absence of such a system, to satisfy orbit stability requirements and reduce beam energy noise, the rf noise will have to be reduced by at least a factor of 3. Specifically, the following numbers are suggested for the rf noise requirements:  $0.075\%$  rms for voltage and  $0.1^\circ$  rms for phase in the band up to 1 kHz.

Table 1: APS-U Beam Orbit Stability Requirements in Frequency Band 0.01 – 1000 Hz

Horizontal	$1.25 \mu\text{m}$	$0.25 \mu\text{rad}$
Vertical	$0.4 \mu\text{m}$	$0.17 \mu\text{rad}$

Similar to decoherence process in transverse plane, one can expect that the decoherence of energy oscillation shown earlier in Fig. 4 could result in increase of the beam energy spread. Figure 7 shows the beam energy spread as a function of the rf phase and voltage modulating frequency. In the presence of energy oscillations, the total beam energy spread is a quadrature sum of the natural beam energy spread and the

contribution of the decoherence effect. Because of the non-zero natural energy spread, the increase of the total energy spread is not large and is limited to frequencies between 100 and 250 Hz. Using this resonance curve and the rf noise from Fig. 1, one can calculate the expected increase in the beam energy spread. The calculations give the total energy spread increase by 7%, which seems negligible.

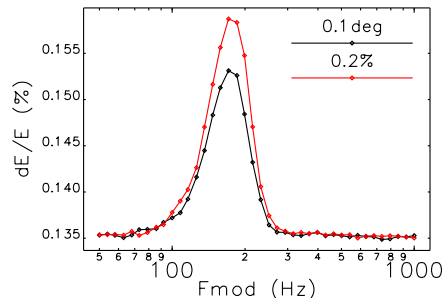


Figure 7: Beam energy spread as a function of rf phase (black) and voltage (red) modulation frequency.

## CONCLUSIONS

We have simulated APS orbit motion due to rf phase modulation using long-term single-particle tracking. We have found that, as expected, the orbit motion follows the equations for a simple damped harmonic oscillator, where damping is the longitudinal synchrotron radiation damping. The analytic solutions for harmonic oscillator agree with tracking simulations very well. One can clearly see the resonance behavior when the phase/voltage modulating frequency approaches the synchrotron frequency.

Since APS-U will utilize a bunch-lengthening higher-harmonic cavity, the analytic solution is harder to find. We used tracking to simulate the effect of the rf modulation on the orbit with the HHC set to “flat-potential” conditions. Similar to APS, we also have found resonance behavior with resonance frequency around 170 Hz but with lower quality factor than that of APS. We used measured rf phase and amplitude noise (Fig. 1) to calculate an expected rms relative beam energy noise of  $4.7 \cdot 10^{-4}$ . This beam energy noise exceeds 30% of the beam energy spread and seems excessive. In addition, this energy noise results in orbit motion that in vertical plane exceeds orbit stability requirements. Reduction of the rf noise by a factor of 3 or more, mostly in voltage stability, would mitigate this. We suggest the following requirements:  $0.075\%$  rms for voltage and  $0.1^\circ$  rms for phase in the band up to 1 kHz. In addition, we looked at the effect of the rf noise on the beam energy spread and found that the expected increase will only be 7%.

## REFERENCES

- [1] M. Borland *et al.*, “The Upgrade of the Advanced Photon Source,” in *Proc. 9th Int. Particle Accelerator Conf. (IPAC’18)*, Vancouver, BC, Canada, May 2018, pp. 2872–2877. doi:10.18429/JACoW-IPAC2018-THXGBD1

- [2] A. Nassiri *et al.*, “An overview of the APS 352-MHz RF systems,” in *Proc. 1997 Particle Accelerator Conf. (PAC’97)*, Vancouver, Canada, May 1997, paper 2P029, pp. 2941–2943.
- [3] T. Berenc, private communication, 2017.
- [4] M. Borland, “elegant: a flexible SDDS-compliant code for accelerator simulation,” Advanced Photon Source, ANL, IL, USA, Rep. ANL/APS LS-287, 2000.
- [5] L. Landau and E. Lifshitz, *Mechanics*, Oxford, UK: Butterworth-Heinemann, 1976.
- [6] H. Wiedemann, *Particle Accelerator Physics*, Berlin, Germany: Springer, 2015.
- [7] S. Kim *et al.*, “Design study of the higher harmonic cavity for Advanced Photon Source upgrade,” in *Proc. 6th Int. Particle Accelerator Conf. (IPAC’15)*, Richmond, Va, USA, May 2015. doi:10.18429/JACoW-IPAC2015-TUPJE076
- [8] M. Kelly *et al.*, “Superconducting harmonic cavity for the Advanced Photon Source upgrade,” in *Proc. 6th Int. Particle Accelerator Conf. (IPAC’15)*, Richmond, Va, USA, May 2015. doi:10.18429/JACoW-IPAC2015-WEPTY008
- [9] A. Hofmann and S. Myers, “Beam dynamics in a double RF system,” CERN, Geneva, Switzerland, Rep. CERN-ISR-TH-RF-80-26, 1980.
- [10] A. Xiao and M. Borland, “Intra-beam and Touschek scattering computations for non-Gaussian longitudinal distributions,” in *Proc. 6th Int. Particle Accelerator Conf. (IPAC’15)*, Richmond, Va, USA, May 2015. doi:10.18429/JACoW-IPAC2015-MOPMA012
- [11] V. Sajaev, “Commissioning simulations for the APS upgrade lattice,” *Phys. Rev. Accel. Beams*, vol. 22, p. 040102, 2019. doi:10.1103/PhysRevAccelBeams.22.040102
- [12] N. S. Sereno, private communication, 2021